

# LMI BASED MULTI-OBJECTIVE $H_\infty$ CONTROL OF FLEXIBLE MICROSATELLITES

C. Pittet<sup>1</sup>, J. Mignot<sup>2</sup>, C. Fallet

CNES, 18 Avenue E. Belin, 31401 Toulouse Cedex 4, France.

## Abstract

In this paper, an applicative example of multi-objective control based on Linear Matrix Inequalities (LMIs) is presented.  $H_\infty$  optimization is used to synthesize a dynamic output feedback controller for a microsatellite subject to disturbances, important sensor time delay, actuator saturation and flexible modes. The reduced controller is compared with classical phase lead controller and finally validated with the complete nonlinear satellite model.

## 1 Introduction

Since the early 90's, the Centre National d'Etudes Spatiales (CNES) has initiated a new and promising field of Research and Technologies dealing with the application of robust control techniques to space activities. In association with industrial and academic partners, the advantages and limitations of robust and linear methods, such as  $H_\infty$  [10] and mixed  $H_2/H_\infty$  optimization [9], [15],  $\mu$ - and  $\nu$ -analysis [16],  $\mu$ -synthesis [10], and the comparison between numerical algorithms using Riccati or LMI formulation, have been widely studied. The suitability of such new techniques has been proven for very various space applications, including microvibration control and attitude control of space vehicles such as satellites and launchers. Today, the numerical efficiency of computers clears most of the obstacles of realization and robust controllers of reduced order are welcome on board.

This paper aims at illustrating the use and validation of robust techniques for the attitude control of a flexible satellite, in a very practical way. In Section 2, the linearized model of the flexible satellite is described, and the performance specification and the closed-loop constraints are given. In the third Section a multi-objective synthesis meeting the performance requirements is proposed, using an  $H_\infty$  optimization based on LMIs to shape the closed-loop transfer functions. The dynamic output feedback is then obtained by using the well-known linearizing change of controller vari-

ables given by Scherer, Chilali and Gahinet [14], [5], [7]. Finally two reduction methods are compared : monovariate simple zero-pole cancellation and Hankel balanced truncation. In Section 4, the closed-loop performance and stability with torque saturation of the actuator are analyzed and compared to the ones with classical phase lead controller, traditionally used for attitude control. Section 5 is devoted to the validation of the controller on the complete attitude control loop simulator of DEMETER microsatellite, with nonlinear dynamics and environmental disturbances, and Section 6 concludes the paper.

**Notations.**  $\mathfrak{R}$  denotes the set of real numbers,  $\mathfrak{R}^n$  denotes the  $n$ -dimensional Euclidean space, and  $\mathfrak{R}^{n \times m}$  denotes the set of all  $n \times m$  real matrices. The notation  $X \geq Y$  (respectively,  $X > Y$ ), where  $X$  and  $Y$  are symmetric matrices, means that the matrix  $X - Y$  is positive semi-definite (respectively, positive definite).  $A'$  denotes the transpose of matrix  $A$ .  $I_n$  denotes the identity matrix in  $\mathfrak{R}^{n \times n}$ . Finally,  $*$  as element  $(i, j)$  of a matrix denotes the transpose of element  $(j, i)$  of the same matrix.

## 2 Problem statement

The microsatellite DEMETER belongs to a new class of satellites developed by CNES, with reduced mass but relevant performances in terms of pointing accuracy (better than 0.1 degree). In order to be autonomous and compliant with different kind of pointing (Earth, Sun or inertial pointing) the attitude measurement is performed by star trackers. The problem with these "intelligent" sensors can be the computation time which can induce a very important time delay in the control loop. Furthermore, the long appendices of the payload generate flexible modes on the platform. Thus the control ensuring band-width requirements, stability and robustness becomes non trivial. For simplicity reasons, a monovariate torque control is considered hereafter.

In order to synthesize the controller, a one axis linear model is derived from the nonlinear dynamics of the satellite. This model can be decomposed into two parts, one rigid body and one flexible structure.

The rigid structure is described by the double integrator equation  $I_r \ddot{\theta} = T$  where  $\theta \in \mathfrak{R}$  is the angular position,  $I_r$

<sup>1</sup>This author is also with LAAS-CNRS, 7 av. Colonel Roche, 31077 TOULOUSE cedex 4, France

<sup>2</sup>Corresponding author. E-mail : jean.mignot@cnes.fr - Fax : +33 (0) 561 27 33 19

is the inertial matrix and  $T \in \mathfrak{R}$  is the external torque.

The flexible mode generates an additional torque  $T_s \in \mathfrak{R}$  on the satellite described by  $T_s = \frac{I_s s^2}{s^2 + 2\zeta\omega_s s + \omega_s^2} \ddot{\theta}$ , where  $I_s = 0.7I_r$  is the inertial matrix of the flexible mode,  $\zeta = 0.005$  its damping ratio, and  $\omega_s = 0.4 \times 2\pi \text{ rad/s}$  its frequency.

Adding a linear Pade approximation to take the time delay (approximately 1 second) induced by the star tracker and the sampling into account, one finally obtains one state space representation of the open-loop system  $G(s)$  :

$$\begin{aligned} \dot{X} &= AX + Bu \\ Y &= CX + Du \end{aligned} \quad (1)$$

with  $X = [\theta \dot{\theta} \eta \dot{\eta} \xi]^T \in \mathfrak{R}^5$ ,  $\eta \in \mathfrak{R}^2$  is the state variable associated to the flexible mode and  $\xi \in \mathfrak{R}$  to the delay,  $u = T \in \mathfrak{R}$ , and  $Y = [\theta \theta_m]^T \in \mathfrak{R}^2$ , where  $\theta_m$  is the delayed angular measurement.

The objectives of the control for any of the three axes are the following :

1. Tracking band-width up to 0.05 Hz
2. Steady-state error less than 0.04 degrees
3. Rejection of additional disturbances on the control input
4. Rejection of the flexible mode gain down to  $-6dB$
5. Control torque limited to  $0.005Nm$

Thus, for each axis, the problem can be expressed this way :

**Problem 1 :** Find a dynamic output controller  $K(s)$  described by

$$\begin{aligned} \dot{x}_c &= A_c x_c + B_c e \\ v &= C_c x_c \end{aligned} \quad (2)$$

meeting the performance requirements 1 to 5, with  $e = \theta_r - \theta_m$  the steady state error ( $\theta_r$  is the angular position reference), and  $v$  the computed control torque.

### 3 LMI synthesis

Because the performance requirements can easily be expressed in terms of gain shaping functions, we have chosen to use loop-shaping  $H_\infty$  methods.

#### 3.1 Loop-shaping

First, let us describe the three shaping transfer functions associated to the specifications.

1.  $W_t(s)$  is devoted to the tracking performance. It also ensures the band-width and the rejection

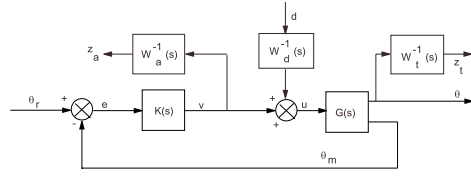


**Figure 1:** Bloc diagram of the augmented system

of the flexible mode for the closed-loop transfer  $\mathcal{T}_t(s) = (1 + G(s)K(s))^{-1}G(s)K(s)$ . In practice, it is a first order low-pass filter, with a  $0dB$  static gain, a  $0.05Hz$  cut-off frequency and a  $-6dB$  gain at the flexible mode frequency.

2.  $W_d(s)$  acts on the input disturbances rejection. It is designed as a low-pass filter, with a  $0dB$  static gain, a  $0.05Hz$  cut-off frequency and a  $-6dB$  gain at the flexible mode frequency. It shapes the transfer function  $\mathcal{T}_d(s) = (1 + G(s)K(s))^{-1}G(s)$ .
3.  $W_a(s)$  ensures both the linearity of the control input within the steady-state error specification (for a suitable domain of initial conditions), and the roll-off of the controller. In practice, we have chosen a second-order low-pass filter, with a  $17dB$  static gain and a  $0.1Hz$  cut-off frequency. It shapes the transfer function  $\mathcal{T}_a(s) = (1 + G(s)K(s))^{-1}K(s)$ .

With these shaping functions, it can be easily shown that Problem 1 is equivalent to :

**Problem 2 :** Find a dynamic output controller  $K(s)$  satisfying  $\|\mathcal{T}_t W_t^{-1}\| \leq 1$ ,  $\|\mathcal{T}_d W_d^{-1}\| \leq 1$  and  $\|\mathcal{T}_a W_a^{-1}\| \leq 1$ .

Actually, it has not been possible to find a solution to this problem, because the constraints are too strict : Problem 2 has to be relaxed. First we have relaxed the tracking performance by allowing an overshoot up to  $3dB$  in the band width. Then we have replaced the feasibility problem by an optimization one.

**Problem 3 :** Find a controller  $K(s)$  solution to  $\min \gamma_t + \gamma_a$  subject to  $\|\mathcal{T}_t W_t^{-1}\| \leq \gamma_t$ ,  $\|\mathcal{T}_a W_a^{-1}\| \leq \gamma_a$ ,  $\|\mathcal{T}_d W_d^{-1}\| \leq 1$ ,  $\gamma_t \geq 1$ , and  $\gamma_a \geq 1$ .

The optimization criterion allows the simultaneous minimization of the overshoot concerning the tracking performance and the constraint on the controller. In order to keep on rejecting the disturbances, constraint  $\|\mathcal{T}_d W_d^{-1}\| \leq 1$  is not relaxed.

#### 3.2 Numerical computation

The numerical computation of the controller will not be totally detailed and the corresponding proofs will not be given here. The computation uses the linearizing

change of variable developed by Scherer [14], Chilali and Gahinet [5], and semi-definite programming.

Let us block-decompose the open-loop system including the shaping functions :

$$\begin{aligned} \dot{x} &= Ax + B_v v + B_r \theta_r + B_d d \\ z_t &= C_t x + D_{tv} v + D_{tr} \theta_r + D_{td} d \\ z_a &= C_a x + D_{av} v + D_{ar} \theta_r + D_{ad} d \\ e &= C_e x + D_{ev} v + D_{er} \theta_r + D_{ed} d \end{aligned} \quad (3)$$

The dimension of this system is 9 (5 for the satellite itself and 4 for the shaping functions). The following theorem states the LMI formulation of the  $H_\infty$  constraints solving Problem 3 :

**Theorem 3.1** : *If there exist positive definite and symmetric matrices  $\mathbb{X}, \mathbb{Y}$  in  $\mathbb{R}^{9 \times 9}$ , matrices  $\mathbb{A} \in \mathbb{R}^{9 \times 9}$ ,  $\mathbb{B} \in \mathbb{R}^{9 \times 1}$ ,  $\mathbb{C} \in \mathbb{R}^{1 \times 9}$ , and positive scalars  $\gamma_t$  and  $\gamma_a$  solutions to :  $\min \gamma_t + \gamma_a$  subject to*

$$\begin{bmatrix} M_1 & * & * & * \\ \mathbb{A} + \mathbb{A}' & M_2 & * & * \\ B'_r & B'_r \mathbb{Y} + D'_{er} \mathbb{B}' & -\gamma_t I_1 & * \\ C_t \mathbb{X} + D_{tv} \mathbb{C} & C_t & D_{tr} & -\gamma_t I_1 \end{bmatrix} < 0 \quad (4)$$

$$\begin{bmatrix} M_1 & * & * & * \\ \mathbb{A} + \mathbb{A}' & M_2 & * & * \\ B'_r & B'_r \mathbb{Y} + D'_{er} \mathbb{B}' & -\gamma_a I_1 & * \\ C_a \mathbb{X} + D_{av} \mathbb{C} & C_a & D_{ar} & -\gamma_a I_1 \end{bmatrix} < 0 \quad (5)$$

$$\begin{bmatrix} M_1 & * & * & * \\ \mathbb{A} + \mathbb{A}' & M_2 & * & * \\ B'_d & B'_d \mathbb{Y} + D'_{ed} \mathbb{B}' & -I_1 & * \\ C_t \mathbb{X} + D_{tv} \mathbb{C} & C_t & D_{td} & -I_1 \end{bmatrix} < 0 \quad (6)$$

$$\begin{bmatrix} \mathbb{X} & I_9 \\ I_9 & \mathbb{Y} \end{bmatrix} > 0 \quad (7)$$

$$\gamma_a > 0.99 \quad (8)$$

$$\gamma_t > 0.99 \quad (9)$$

with matrices  $M_1 = \mathbb{A}\mathbb{X} + \mathbb{X}\mathbb{A}' + B_v \mathbb{C} + \mathbb{C}' B'_v$  and  $M_2 = \mathbb{Y}\mathbb{A} + \mathbb{A}'\mathbb{Y} + \mathbb{B}\mathbb{C}_e + \mathbb{C}'_e \mathbb{B}'$ , then the controller described by :

$$\begin{cases} C_c = \mathbb{C}(M')^{-1} \\ B_c = N^{-1}\mathbb{B} \\ A_c = N^{-1}(\mathbb{A} - \mathbb{Y}\mathbb{A}\mathbb{X} - \mathbb{Y}B_v\mathbb{C} - \mathbb{B}\mathbb{C}_e\mathbb{X} - \mathbb{B}D_{ev}\mathbb{C})(M')^{-1} \end{cases} \quad (10)$$

where  $M$  and  $N$  belongs to  $\mathbb{R}^{9 \times 9}$  such that  $\mathbb{X}\mathbb{Y} - I_9 = -MN'$ , solves Problem 3.

**Proof** : LMIs (4), (6) and (5) come from the Bounded Real Lemma [2], [7] applied to the closed-loop system with the shaping functions. By using the linearizing change of controller variables, it is readily shown that LMI (4) corresponds to  $\|\mathcal{T}_t W_t^{-1}\| \leq \gamma_t$ , LMI (5) corresponds to  $\|\mathcal{T}_a W_a^{-1}\| \leq \gamma_a$  and LMI (6) means  $\|\mathcal{T}_d W_d^{-1}\| \leq 1$ . LMI (7) ensures the existence of a Lyapunov function for the closed-loop system, so its stability. Finally, by using the inverse linearizing change of variables, one gets the matrices given by (10).

**Remark 3.1** : *Assuming that there exists matrices  $\mathbb{A}, \mathbb{B}, \mathbb{C}, \mathbb{X}$  and  $\mathbb{Y}$  satisfying LMIs (4), (6), (5) and (7) of*

*Theorem 3.1, then matrices  $M$  and  $N$  do always exist. Note that  $M$  and  $N$  are not unique, and the stability of the controller depends on the decomposition method used to compute them. In this example, we have added conditioning constraints on LMI (7) so that  $\mathbb{X}\mathbb{Y} - I$  is negative enough, and we have used the matricial square root decomposition function `SQRTM.m` of `MATLAB`.*

**Remark 3.2** : *Theorem 3.1 is not specific to the monovariate case, and can be used directly for multivariate system and multivariate shaping functions. The difficulty is in the choice of these functions to meet the performance requirements.*

**Remark 3.3** : *If no solution exists satisfying Theorem 3.1, then the shaping functions must be modified or the  $H_\infty$  constraints must be relaxed.*

The controller dimension is equal to the dimension of the open-loop system including the shaping functions (3), so it is often very large. In our case, the satellite system (1) is of order 5 (with delay and flexible mode), the shaping functions add 4 state variables, so the controller order is 9. Now, this order has to be reduced.

### 3.3 Controller Reduction

The idea is to eliminate high frequency useless dynamics and flexible mode cancellation. This allows to keep the low frequency behavior of the controller and ensures its robustness as far as the flexible mode is concerned. We can compare two open-loop methods : zero-pole like cancellation, and Hankel balanced truncation with static gain keeping [15].

- **Zero-pole like cancellation.** This is an iterative manual reduction based on cancellation of close dynamics of the numerator and denominator. The controller denominator and numerator are decomposed in elementary first and second order filters. Then the cells are cancelled, and either the static gain, or the high frequency behavior (integrator or derivator) are kept. This is an heuristic method and the cancellation needs to be validated at each iteration by comparing the closed-loop performances and the stability margins with and without reduction.

- **Hankel truncation.** This is another open-loop reduction method, but more systematic. Indeed, the only parameter that the user needs to choose is the final order of the reduced controller. The truncation itself is automatic. It uses the grammians information. The less observable and controllable modes are eliminated. The drawback of this method is that it generates non-strictly proper controllers. Thus we cancel manually a zero at the end. The result is *a priori* different from the last method, because the reduced controller does

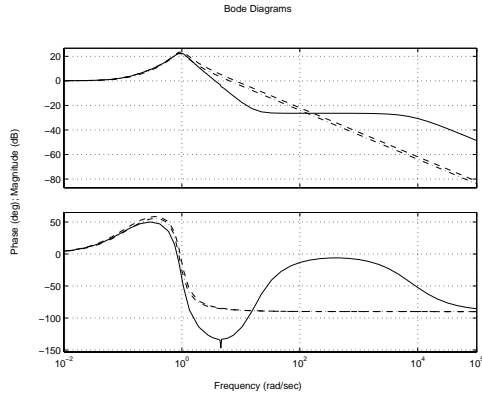


**Figure 2:** Full-order, Manually reduced ('- -'), Hankel reduced ('-.-') controller

not have strictly the same eigenvalues as the full-order one.

Figure 2 shows that the reduced controllers are very similar, which proves that both reduction methods are equivalent for this example. The behavior of both closed-loop systems is the same. We can notice that the controller behaves as a phase lead filter, which is the classical controller for attitude control.

#### 4 Comparison

We have synthesized a phase lead controller with classical methods in order to compare it with our  $H_\infty$  controller, in terms of stability, performance and robustness. The control loop with classical phase lead filter is slightly different. It includes a given derivative filter in the feedback loop, and the control is driven by a static gain on the angular reference error, and a low-pass first order filter on the velocity reference error. This loop is described on Figure 3.

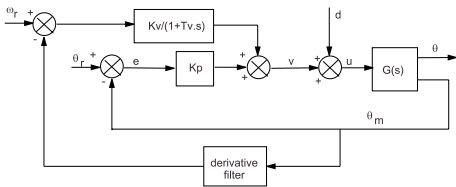


**Figure 3:** Phase lead control loop

A convenient controller is obtained via classical methods with  $K_p = 2$ ,  $K_v = 7.2$ , and  $T_v = 0.4$ .

##### 4.1 Stability analysis

The first comparison criterion is the closed-loop stability with torque saturation of the input control. Because of the double integrator in the open-loop system and of the controller linearity, the closed-loop stability

is ensured only in a bounded domain around the equilibrium point [6], [8]. The exact domain of stability is very difficult to find analytically. In order to overcome this difficulty, we search for an approximation of the stability region, as large as possible. For simplicity reasons, the approximated domain of stability is of ellipsoidal form, and the saturation of the closed-loop will not be allowed. For each controller, the analysis algorithm providing the maximized domain of stability is the following :

##### Algorithm 4.1

1. Isolate the saturating term of the interconnected system (made of satellite and controller), described by matrices  $\mathbf{A}$ ,  $\mathbf{B}$ ,  $\mathbf{F}$ , such that the closed-loop system can be rewritten as the following saturated system :

$$\dot{\mathbf{X}} = \mathbf{A}\mathbf{X} + \mathbf{B}\text{Sat}(\mathbf{F}\mathbf{X}) \quad (11)$$

where  $\text{Sat}(\mathbf{F}\mathbf{X})$  is defined by :

$$\text{Sat}(\mathbf{F}\mathbf{X}) = \begin{cases} -0.005 Nm & \text{if } \mathbf{F}\mathbf{X} < -0.005 Nm \\ \mathbf{F}\mathbf{X} & \text{if } |\mathbf{F}\mathbf{X}| \leq 0.005 Nm \\ 0.005 Nm & \text{if } \mathbf{F}\mathbf{X} > 0.005 Nm \end{cases}$$

2. Solve the following optimization problem : minimize  $\mu$  such that the ellipsoidal set  $\mathcal{E} = \{\mathbf{X} : \mathbf{X}'\mathbf{P}\mathbf{X} \leq \mu^{-1}\}$  is included in the hyperplane defined by  $\mathcal{S} = \{\mathbf{X} : |\mathbf{F}\mathbf{X}| \leq 0.005\}$  and  $\mathbf{P}$  is a positive definite and symmetric matrix, solution of the Lyapunov inequality  $(\mathbf{A} + \mathbf{B}\mathbf{F})'\mathbf{P} + \mathbf{P}(\mathbf{A} + \mathbf{B}\mathbf{F}) < 0$

Then, any trajectory of the closed-loop system, initiated in the ellipsoid  $\mathcal{E}$  remains in the linear domain  $\mathcal{S}$  (where no saturation occurs), and tends to the equilibrium point as time  $t$  tends to infinity. The numerical computation is made via an LMI formulation [13], [3], [4]. The results are shown on Figure 4 : the smaller ellipsoid corresponds to the classical phase lead controller. We can see that the  $H_\infty$  controller provides a larger domain of stability for the closed-loop system.

**Remark 4.1 :** The stability domain can be taken into account within the synthesis algorithm via an LMI formulation. Indeed, it is possible to add LMI constraints to make sure that the ellipsoidal domain of stability includes a specific domain of initial conditions [12]. However, the use of a unique Lyapunov function for the performance requirements and the stability constraints makes this synthesis conservative. There is actually a trade-off between the performance and the size of the stability domain. The analysis generally provides larger domains of stability.

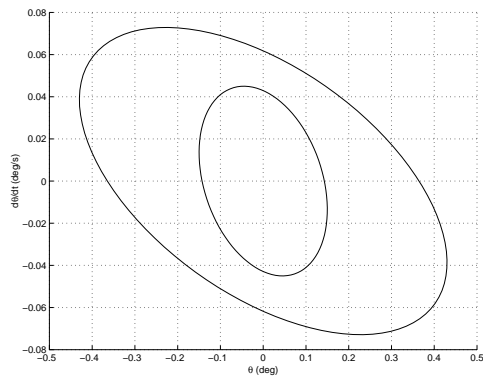


**Figure 4:** Projection of the stability domains on the  $(\theta, \dot{\theta})$  hyperplane

## 4.2 Performance improvement

As far as the closed-loop system remains linear, the performance is related to its eigenvalues. If we analyze the rigid body ones, we can notice that the  $H_\infty$  controller provides globally faster and more damped dynamics than the classical phase lead. The slowest and less damped eigenvalues corresponding to the flexible mode are not cancelled nor controlled in order to ensure the robustness against modelling errors. Thus, they still appear on both loops.

## 4.3 Robustness analysis

Many parameters of the open-loop model are not definitively fixed and modelling errors can be important. Thus the parameters are rather defined inside an interval.

In order to illustrate the parametric robustness of both closed-loops, we propose to detail a  $\mu$ -analysis with uncertainty on the frequency of the flexible mode [15]. Let us consider the frequency  $\omega_s = (1 + \delta)\omega_{s0}$ , where  $\omega_{s0}$  is the nominal frequency, and  $|\delta| < 1$  is the real uncertainty. The dynamic equation of the flexible mode is given by :

$$\sqrt{I_s}\ddot{\theta} + \dot{\eta} + C_s\dot{\eta} + K_s\eta = 0$$

with  $C_s = (1 + \delta)C_{s0}$ , and  $K_s = (1 + \delta)^2K_{s0}$  respectively the friction and stiffness. Let us introduce two additional outputs  $z_1$  and  $z_2$  and two inputs  $\nu_1$  and  $\nu_2$ , such that  $\nu_1 = \delta z_1$ ,  $\nu_2 = \delta z_2$ ,  $z_1 = K_{s0}\eta$  and  $z_2 = 2K_{s0}\eta + s\nu_1 + C_{s0}\dot{\eta}$ . Then the flexible mode equation becomes :

$$\sqrt{I_s}\ddot{\theta} + \dot{\eta} + C_{s0}\dot{\eta} + K_{s0}\eta + \nu_2 = 0$$

This writing separates the nominal plant from the uncertainty, which is isolated in the additional loop defined by  $\nu = \Delta z$ , with  $\nu' = [\nu_1 \ \nu_2]$ ,  $z' = [z_1 \ z_2]$  and  $\Delta = \begin{bmatrix} \delta & 0 \\ 0 & \delta \end{bmatrix}$ .

Then, we can show that the admissible interval for frequency  $\omega_s$  is given by  $\max |\omega_s - \omega_{s0}| = \frac{1}{\min_\omega(\mu(\omega))}$  where  $\mu$  is the structured singular value of the closed-loop nominal system. By using the MATLAB function MU.m, we find a maximal bound of  $\mu$ , and thus a minimal bound of the variation interval. For the classical phase lead controller, the admissible variation is  $\delta_{max} = 0.22$  (so  $\omega_s$  can be between 0.31 and 0.49 Hz), whereas with the  $H_\infty$  controller, it grows up to  $\delta_{max} = 0.35$  (so  $\omega_s$  can be between 0.26 and 0.54 Hz). This proves the robustness of the  $H_\infty$  controller.

## 5 Numerical simulation with nonlinear satellite model

The final acceptance of an attitude control law depends on its performance and behavior within the nonlinear closed-loop. There, the satellite model includes many nonlinearities, such as vectorial products induced by the driving velocities and accelerations. Furthermore, it includes persistent input and measurement noise. Finally, the model includes inertial coupling and 8 flexible modes. In order to use this complex model, we have synthesized an  $H_\infty$  and a classical phase lead controller for each axis, and we have put the decoupled controllers in the simulator. The closed-loop is described on Figure 5.

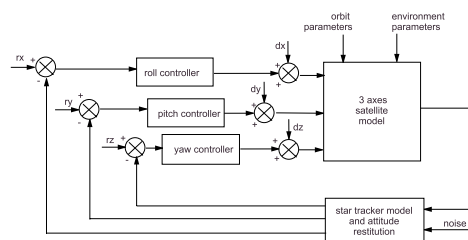


**Figure 5:** Block diagram of the nonlinear closed-loop system

We have compared the tracking performance obtained with phase lead and  $H_\infty$  controllers. The result is shown on Figure 6. Initial pointing error is set to 0.01 deg for each axis. It is clear that the  $H_\infty$  time response is smaller. The stability is verified for both systems. Finally, this simulation with the nonlinear model shows that each axis can be controlled independently, and that one axis control is suitable.

**Remark 5.1** *The bias on the Y axis is due to the orbital coupling : instead of a step reference input, the Y reference signal is a ramp whose slope is the orbital frequency ( $\omega_0 = 0.001\text{rad/s}$ ). We can show that the ramp error is equal to  $\omega_0 T_r$ , where  $T_r$  is the time delay.*

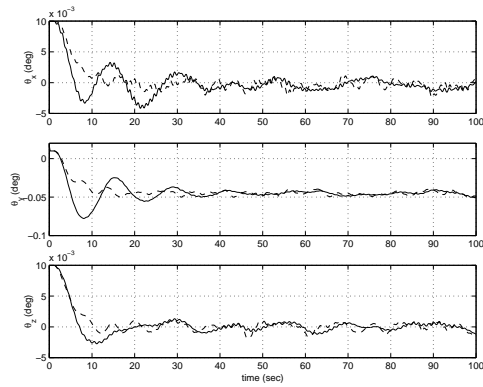


**Figure 6:** Nonlinear closed-loop system simulation : '- -'  $H_\infty$ , '-' phase lead controllers

## 6 Conclusion

In this paper, we have detailed the synthesis of robust  $H_\infty$  controller for the decoupled attitude control of a flexible microsatellite. First we have seen how the performance requirements (tracking, band-width, flexible mode rejection, non saturation of reaction wheel) can be expressed in terms of loop-shaping of the closed-loop transfers. Then we have described the LMI-based synthesis algorithm using a linearizing change of controller variables [14], [5]. Next, the reduction operated manually or via Hankel balanced truncation has been explained, and we have shown that both methods lead to equivalent controllers. A comparison with classical phase lead controller shows that the  $H_\infty$  controller provides better results, in terms of size of the stability domain without reaction wheel saturation, of time response and damping, and finally of parametric robustness. Finally, this comparative result has been confirmed on the nonlinear and coupled simulation model.

This successful application illustrates the benefits of new techniques of control for space applications. The use of the LMI formulation makes the synthesis easier and it would be interesting to extend the multi-objective synthesis. A short term research axis could include multivariable control for coupled systems or for combining position and velocity feedbacks,  $H_2$  optimization for noise rejection, pole placement in LMI regions in order to control the time response, stability margins, and damping of the closed-loop system. A longer term research axis could be the stabilization with rate or integral saturations for a better modelling of the actuators behavior, reduced fixed-order controller synthesis, or LPV control, which could allow the control of the satellite during the changes of operationnal modes.

## References

[1] D.S. Bernstein and A.N. Michel : *Special issue : Saturating actuators*, Int. J. of Robust and Nonlinear

Control, vol.5, pp.375-540, 1995.

[2] S. Boyd, L. El Ghaoui, E. Feron, V. Balakrishnan: *Linear Matrix Inequalities in System and Control Theory*, SIAM studies in Applied Mathematics, Philadelphia (USA), 1994.

[3] C. Burgat and S. Tarbouriech : *Nonlinear Systems*, Vol.2, Chapter 4, pp.113-197, Appendices C, D, E, pp.217-239, Chapman & Hall, London, 1996.

[4] C. Burgat, S. Tarbouriech and M. Klai: *Continuous-time saturated state feedback regulators-Theory and design*, Int. J. Syst. Sci., vol.25, no.2, pp.315-336, 1994.

[5] M. Chilali and P.Gahinet :  *$H_\infty$  design with pole placement constraints : an LMI approach*, IEEE Trans. Autom. Control, vol.41, no.3, pp.358-367, 1996.

[6] A.T. Fuller : *In the large stability of relay and saturated controls systems with linear controller*, Int. j. Contr., 10, pp.457-480, 1969.

[7] P. Gahinet : *Explicit controller formulas for LMI-based  $H_\infty$  synthesis*, Automatica., vol.32, pp.1007-1014, 1996.

[8] H.K. Khalil : *Nonlinear system*, Macmillan Ed., 1992.

[9] E. Magarotto, B. Frapard, R. Fayard, M. Zasadzinski, J. Mignot :  *$H_2/H_\infty$  control design : LMI techniques for space applications*, Proc. Conf. Contr. and Applic., Trieste, Italy, 1998.

[10] D. Martinez :  *$H_\infty$  design and  $H_\infty$  control of GAMMA bench*, Proc. EUROMECH Conf. 341, september 1995.

[11] B.C. Moore : *Principal components analysis in linear systems : controllability, observability and model reduction*, IEEE Trans. Autom. Control, AC, 26, n.1, pp.17-31,1981.

[12] C. Pittet, S. Tarbouriech, C. Burgat : *Output feedback synthesis via the circle criterion for linear systems subject to saturating inputs*, Proc. 37th IEEE Conference on Decision and Control (CDC 98), TAMPA, USA, pp.401-406, 1998.

[13] C. Pittet : *Stabilization of systems with constrained inputs, application to a microdynamic excitation table*, Ph.D. report, University Paul Sabatier, n. 3077, LAAS report n.98434, October 1998.

[14] C.W. Scherer : *From LMI analysis to multichannel mixed LMI synthesis : a general procedure*, Selected Topics in Identification, Modelling and Control, vol.8, pp.1-8, 1995.

[15] C. Valentin-Charbonnel : *Commande robuste avec contrainte d'ordre, par la norme  $H_\infty$  et le formalisme LMI. Application au contrôle d'attitude d'un satellite d'observation de la Terre*, Ph.D. report, University Paris XI ORSAY, n.5478, 1998.

[16] C. Valentin, G. Duc, S. Le Ballois : *Robust control of a satellite axis : low order  $H_\infty$  design and  $\nu$ -analysis*, 2nd Symposium on Robust Control Design (ROCOND), Budapest, pp.441-446, 1997.